

Impact of ferulic acid and resveratrol on the effectiveness and safety of sunscreen

Thamires Batello Freire¹, Claudinéia Aparecida Sales de Oliveira Pinto¹,
Maria Inês de Almeida Gonçalves¹, Cristina Helena dos Reis Serra¹,
Michelli Ferrera Dario^{1*}, André Rolim Baby¹, Maria Valéria Robles Velasco¹

¹Department of Pharmacy, School of Pharmaceutical Sciences,
University of São Paulo, São Paulo, Brazil

The combination of avobenzone (AVO) and octyl ρ -methoxycinnamate (OMC) is widely used to ensure broad-spectrum photo-protection because they absorb UVA and UVB, respectively. However, they are thermally and photo unstable because they degrade and undergo photo-tautomerization and *trans*-*cis* isomerization, thus reducing their photo-protection efficacy during UV exposure. This study aimed to evaluate the potential use of the antioxidants ferulic acid and resveratrol as stabilizing substances in AVO and OMC mixtures in solution or emulsion. The effects of both antioxidants on the thermal/photo-stability and suppression of the filter singlet state, besides skin permeation, were evaluated. Both antioxidants contributed to preserving OMC and AVO during the thermal stability test, which relates to the maintenance of photo-protection even after storing the formulations at high temperatures. Nevertheless, although resveratrol retained part of the OMC *trans* isomer and suppressed the AVO singlet state when exposed to UV, no contribution to photo-protection stability was observed, contrary to expectations. Regarding the permeation assay, the addition of both antioxidants was accompanied by a reduction of AVO permeation, while resveratrol increased OMC permeation. Thus, the chemical and physicochemical properties of these antioxidants impacted their efficacy and safety profiles; therefore, further studies are required to establish the real cost-benefit ratio for their use in sunscreens.

Keywords: Ferulic acid. Resveratrol. Antioxidants. Permeation. Sunscreen.

INTRODUCTION

Prolonged skin exposure to UV radiation causes deleterious effects on health and aesthetics, such as premature aging, pigmentation changes, inflammation, and carcinoma. An estimated 10% reduction in ozone layer levels would result in an additional 300,000 and 4,500 cases of nonmelanoma and melanoma skin cancer, respectively (WHO, 2017). Furthermore, damage to the epidermal barrier caused by UV exposure alters tight junction protein expression and decreases covalently bound ceramides in stratum corneum thereby increasing

its thickness and transepidermal water loss (TEWL) (Barresi *et al.*, 2021).

Sunscreens need to be photo-stable to provide effective protection against UV rays. Without this ability, they can degrade and photo-allergic reactions can occur on human skin (Serpone, 2021). An association between the low photo-stability of organic filters and their ability to remain in the triplet energy state (three quantized states) is mentioned in the literature. Thus, it is necessary to return to the fundamental state for sunscreen to continue absorbing energy (Herzog, Giesinger, Settels, 2020)

Chemical filters such as avobenzone (*butyl methoxydibenzoylmethane*; AVO) and octyl ρ -methoxycinnamate (*ethylhexyl methoxycinnamate*; OMC) are widely used in photo-protective formulations. The AVO filter was introduced into the market in the late

*Correspondence: M. F. Dario. Departamento de Farmácia. Faculdade de Ciências Farmacêuticas. Universidade de São Paulo. Avenida Prof. Lineu Prestes, 580, BI-13/15. CEP.: 05508-000, São Paulo, SP, Brasil. Phone: 55 11 3091-3623. E-mail: mfdario@gmail.com. ORCID: <http://orcid.org/0000-0002-0050-4378>

1980s and early 1990s and was the first to offer protection against UVA rays (315–400 nm). When exposed to UV radiation, AVO is substantially degraded through photo-tautomerization to its ketone form, which partially favors the loss of its ability to absorb in the UVA range (Berenbeim *et al.*, 2020). The OMC filter was developed in the 1950s and is popular in the US and Europe. It absorbs UVB rays (280–315 nm), but upon exposure to UV radiation, *trans*–*cis* isomerization can occur, making it less effective (Herzog *et al.*, 2019).

Although chemical filters have been used for decades, their safety, efficacy, and toxicological profiles remain unclear. There is growing concern regarding the potential harmful consequences of skin exposure to OMC, AVO, and other chemical filters, considering their cutaneous permeation, possibility of absorption, and interference with the human endocrine system. These behaviors can interfere with the photo-protective efficacy and safety of sunscreen (Jiménez *et al.*, 2004; Klimová, Hojerová, Beránková, 2015).

The addition of photo-stabilizers is convenient to avoid reactions that decrease the photo-stability of the chemical filters. Studies regarding the use of antioxidants with natural origins have been conducted to determine effective and safe formulations. Ferulic acid (FA) and resveratrol (RES) have been reported as antioxidants with natural origins and may also have UV absorption properties, which justifies their incorporation in multifunctional sunscreens. In addition, there is the possibility of synergism with chemical filters, which may reduce the UV filter concentrations needed (Peres *et al.*, 2018; Rojas, Londono, Ciro, 2016). This study aimed to evaluate the safety and efficacy of sunscreens associated with FA and RES, especially regarding their photo-stability and skin permeation.

MATERIAL AND METHODS

Chemicals

RES with 99.8% purity was obtained from Active Pharmaceutica (Brazil), FA with 98.6% purity was obtained from GAMMA (Brazil), AVO and OMC with 98.2% and 98.6% purity, respectively, were obtained

from Fagron (Brazil). Analytical standard dimethylsulfone was purchased from Sigma–Aldrich (USA). Monobasic sodium phosphate and sodium hydroxide were obtained from Synth. Tetramethylsilane and dimethylsulfoxide- d_6 (DMSO) with 99.8% purity were obtained from CIL (USA). Bovine serum albumin with 98.0% purity (bovine serum albumin [BSA], fraction V) was purchased from Inlab (Brazil) and ethyl acetate was purchased from Alpax (Brazil). Phenylethyl benzoate was purchased from ISP (Brazil). High-performance liquid chromatography (HPLC) grade methanol and chloroform- d_6 with 99.8% purity were obtained from Merck (Germany).

Molecular stability of chemical filters

Exactly 240 mg AVO, 480 mg OMC, 30 mg FA or RES, and 60 mg dimethylsulfone (internal standard) were transferred to a 3.0 mL quartz cuvette, followed by the addition of DMSO- d_6 . Aliquots of 0.5 mL were transferred to analytical nuclear magnetic resonance (NMR) tubes before and after UV exposure (Batista *et al.*, 2008).

UV irradiation was performed by using a Suntest® CPS+ solar simulator (Atlas, Germany), fitted with a Daylight filter, for 2, 4, and 6 h (maximum total UV dose 1564 KJ.m⁻²) and irradiance of 72.4 W.m⁻² (320–400 nm). Solutions comprised of chemical filters and antioxidants were exposed to UV radiation in quartz cuvettes with a 1 cm optical path (Herzog *et al.*, 2019).

The ¹H NMR spectra for the quantitative determination of the filters were obtained in a Bruker (Rheinstetten/Karlsruhe, Germany), DPX300® Spectrometer with a 5 mm multinuclear probe at 300.13 MHz (¹H), high-performance digital Fourier Transform Nuclear Magnetic Resonance (FT-NMR). The following parameters were optimized for qNMR: 30° pulse, preacquisition delay of 5 μs, relaxation delay of 10 s, and a total of 32 scans. The NMR probe temperature was maintained at 30°C and chemical shifts were referenced internally to tetramethylsilane (TMS = 0.0). Data processing was performed using the Fourier transform with a 0.3Hz exponential filter. Phase and baseline corrections were manually adjusted, as well as the integration of signals, thereby avoiding the integration of the ¹³C satellite peaks (Pinto *et al.*, 2021).

The equilibrium constants of the OMC isomers (*trans/cis*) and AVO tautomers (enol/keto) (Figure 1) were calculated according to Equation 1 (Holzgrabe *et al.*, 2005).

$K = \% \text{ unmodified filter} / \% \text{ modified filter}$ (Equation 1)

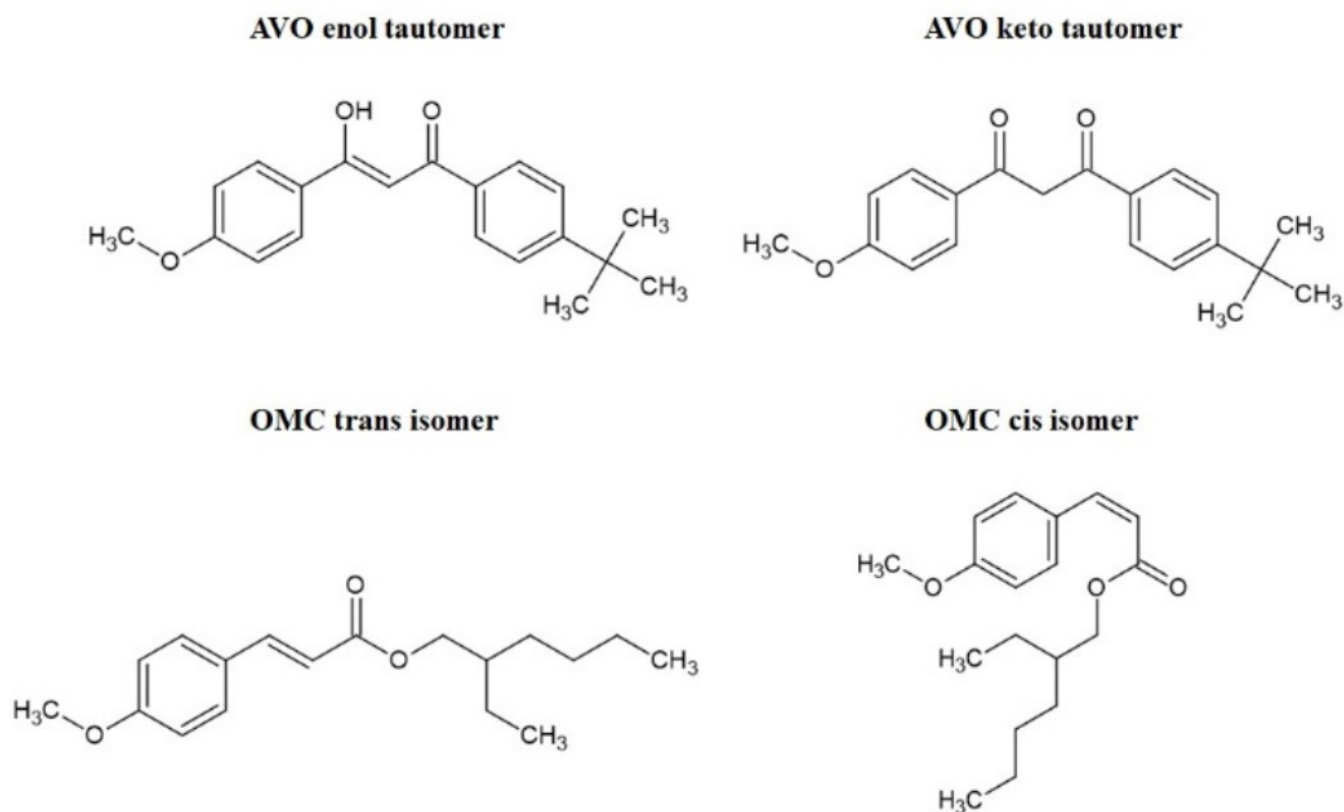


FIGURE 1 - Structural formulas of Avobenzone (AVO) and Octyl *p*-methoxycinnamate (OMC).

Qualitative analysis of singlet energy state suppression

Suppression of the singlet energy state was qualitatively evaluated by observing the fluorescence of AVO and OMC in isolation or combination with the antioxidants (FA or RES) in methanol solution. Phenylethyl benzoate was used as the negative control. The solutions (10 μL) were transferred to a chromatoshet of silica gel containing a fluorescent indicator. The fluorescence was analyzed under 365 nm excitation and the response was considered positive when the samples showed decreased fluorescence compared with the negative control (Bonda, 2009).

Photo-protective formulations

Oil-in-water (O/W) emulsions were formulated according to Table I. The concentration of the chemical filters was with the recommended limits of Agência Nacional de Vigilância Sanitária (ANVISA, Brazil) (Anvisa, 2022) and European Union Cosmetics Regulation 1223/2009 (Union, 2009). The formulation components were heated at 75.0°C, followed by mechanical agitation at 1000 rpm during cooling step. The preservative (parabens) and antioxidants FA and RES were added at 40°C.

TABLE I - Formulation composition

Ingredients (*INCI)	% w/w		
	BF	BF + FA	BF + RES
Ammonium acryloyl-dimethyltaurate/VP copolymer	1.0	1.0	1.0
Propyleneglycol	10.0	10.0	10.0
Cetearylalcohol (and) dicetylphosphate (and) ceteth-10 phosphate	10.0	10.0	10.0
Caprylic/capric acid triglyceride	10.0	10.0	10.0
Butyl methoxydibenzoylmethane	5.0	5.0	5.0
Ethylhexyl methoxycinnamate	10.0	10.0	10.0
Phenoxyethanol (and) methylparaben (and) ethylparaben (and) butylparaben (and) propylparaben (and) isobutylparaben	0.7	0.7	0.7
Resveratrol	-	-	3.0
Ferulic acid	-	1.0	-
Aqua added to make up	100.0	100.0	100.0

Legend: INCI, International Nomenclature of Cosmetic Ingredient; BF, base formulation; FA, ferulic acid; RES, resveratrol.

Thermal stability evaluation

Photo-protective formulations were stored under different temperature conditions: $5.0 \pm 2.0^\circ\text{C}$, $20.0 \pm 2.0^\circ\text{C}$, and $45.0 \pm 2.0^\circ\text{C}$ for 90 d. Formulations were analyzed at t_0 (48 h after preparation) and t_{90} (at the end of the storage period) according to the following parameters: *in vitro* photo-protective efficacy (estimated SPF – sun protection factor), $\lambda_{\text{critical}}$, and UVA/UVB ratio) and chemical filter concentrations. The photo-protective efficacy was assessed using a diffuse reflectance spectrophotometer equipped with an integrating sphere (Labsphere® UV-2000S Ultraviolet Transmittance Analyzer), and quantification of the chemical filters was performed by qNMR as described above.

In vitro photo-protective evaluation

The estimated SPF, $\lambda_{\text{critical}}$, and UVA/UVB ratio were determined in a Labsphere® UV200S, between 290 and 400 nm, and at every 1.0 nm the mean of three plate readings for each sample were considered,

with 9 readings at the different points. Formulations were uniformly applied as a film on the surface of polymethylmethacrylate (PMMA) (Helioplate® HD6) at $1.3 \text{ mg}\cdot\text{cm}^{-2}$, in circular movements and dried for 30 min at room temperature ($25.0 \pm 2.0^\circ\text{C}$). A PMMA plate with glycerin was used as the blank.

Chemical filter quantitative analysis by ¹H-NMR

An aliquot of 0.8 g formulation was added to 1.0 mL CDCl_3 , vortexed for 5 min, and centrifuged for 15 min at 10,000 rpm to separate any insoluble material. The supernatant was discarded, the remaining solution was mixed with 20 mg of dimethylsulfone (internal standard), and the volume was made up to 1.0 mL with CDCl_3 . Solutions were transferred to NMR analytical tubes, and analyses were performed as described above. The amount of chemical filter was quantified according to Equation 2 (Zhang *et al.*, 2021).

$$\frac{m(a)}{m(IS)} = \frac{A(a)}{A(IS)} \times \frac{N(IS)}{N(a)} \times \frac{M(a)}{M(IS)} \times (IS) \text{purity} \quad (\text{Equation 2})$$

where: $m(a)$ is the mass of the analyte; $m(IS)$ is the mass of the internal standard; $A(a)$ is the analyte signal area; $A(IS)$ is the internal standard signal area; $N(IS)$ is the number of hydrogen nuclei present in the signal of the internal standard; $N(a)$ is the number of hydrogen nuclei present in the analyte signal; $M(a)$ is the analyte molar mass; $M(IS)$ is the internal standard molar mass, and (IS) is the internal standard purity (98.0%).

Photo-stability of photo-protective formulation

Formulations with an $SPF \geq 15$ and $\lambda_{critical} \geq 370$ nm were irradiated in the Suntest® CPS+ solar simulator (Atlas, Germany). The emission was maintained at $47.6 \text{ W}\cdot\text{m}^{-2}$ (320–400 nm), and the total dose of incident radiation was $85.68 \text{ kJ}\cdot\text{m}^{-2}$. The photo-protective efficacy parameters (*in vitro* SPF, $\lambda_{critical}$, and UVA/UVB ratio) were determined according to the aforementioned methodology before and after exposure to UV radiation at time points t_0 and t_{90} (during stability evaluation).

In vitro skin permeation

In vitro percutaneous permeation of the chemical filters was performed using jacketed Franz diffusion cells (Freitas *et al.*, 2015). Porcine ear skin was used as a model for human skin permeability after approval was provided by the local Ethics Committee (Protocol n° 553 CEUA/FCF/USP). Before the study, the porcine ears subcutaneous cartilage was removed, and the skin was cleaned with water and a neutral detergent. The skin was maintained at -5.0°C until use. Aliquots of 150 mg formulation were applied to a 1.77 cm^2 diffused area on the skin surface and repeated in triplicate. The receptor fluid (phosphate buffered saline (PBS) pH 7.4 with 4.0% BSA) was maintained at 37.0°C using a jacketed Franz's cell and magnetic stirrer. Aliquots of receptor fluid were taken at 4 and 24 h, and the volume removed was replaced with an equivalent volume of fresh receptor fluid.

At the end of the permeation study, the excess formulation was gently removed from the skin surface with a swab. The skin was submitted to the tape stripping technique, and chemical filters were quantified at the

tapes (stratum corneum) and epidermis plus dermis. The stratum corneum was removed by applying Scotch® 3M magic transparent adhesive tape ($1.5 \times 1.0 \text{ cm}$) 15 times over the skin area. The first tape was quantified separately due to the possibility of it containing remnant formulation. After removing the stratum corneum, the skin (epidermis plus dermis) was cut into small fragments and transferred to falcon tubes with 6 mL methanol. Samples were vortexed for 5 min and sonicated for 5 min to break the cells and extract the studied substances. After appropriate dilution, the samples were filtered through $0.45 \mu\text{m}$ pore filters and analyzed by HPLC.

HPLC chromatographic conditions

Organic filters were quantified in a Shimadzu® LC-20AD/T chromatograph using a C18 column ($150 \times 4.6 \text{ mm}$, 3 mm particle size) with a guard column ($10 \times 4.6 \text{ mm}$), detector diode-array UV detector. The previously validated method consisted of ultrapure water:methanol (12:88) as the mobile phase, a flow rate of $0.8 \text{ mL}/\text{min}$, and a $10 \mu\text{L}$ injection. The detection was performed at 325 nm and 25.0°C . All samples were filtered through $0.45 \mu\text{m}$ pore filters before injection.

Statistical analysis

Results were statistically analyzed using one-way analysis of variance followed by Tukey's Multiple Comparison Test, *t*-test for two means or paired *t*-test using the Minitab® 17 1.0 software ($\alpha = 0.05$).

RESULTS AND DISCUSSION

Photo-stability of the organic filter solutions

Sunscreen formulations must contain UVB and UVA filters to protect the skin from sun-induced disorders such as erythema, skin cancer, and photo-aging. However, these formulations should be photo-stable since they are constantly exposed to sun radiation. AVO is the most widely used UVA filter in cosmetic sunscreens, although this photo-excited molecule transforms into several transient tautomeric forms and the keto-tautomer

is responsible for its photo-degradation (Herzog, Giesinger, Settels, 2020). In the base state, AVO is mostly found in its enol form due to stabilizing intramolecular hydrogen bonds (Berenbeim *et al.*, 2020). Thus, keto–enol tautomerization and photo-degradation explain the reduction in UVA protection of AVO under irradiation conditions (Kojic, Petkovic, Etinski, 2016).

The solution containing OMC and AVO filters had lower *trans/cis* and enol/keto ratios, respectively, as the dose increased, thus denoting its loss of efficacy after irradiation (Table II). Under a 1564 kJ.m⁻² irradiation dose, the *trans/cis* ratio for OMC was 3.96 and the enol/

keto ratio for AVO was 9.31. The nonconservation of the *trans* and enol forms for OMC and AVO, respectively, indicates the UV absorption efficiency of the chemical filters. The higher the ratio value, the greater the photostability. The signals generated by the selected hydrogens were detected at 4.72 and 7.18 ppm for the ketone and enol forms of the AVO and at 5.83 and 6.44 for the *cis* and *trans* OMC, respectively. Murphy *et al.* (2020) obtained the AVO enol read at 7.23 in DMSO-d₆. They also observed two major and minor peaks beyond two doublets for AVO in the aromatic region, which may indicate the ortho-resonances of the phenyl ring.

TABLE II - Quantification of molecular changes of AVO and OMC filters with or without the addition of FA or RES in DMSO-d₆ solution after exposure to UV radiation

Solution	UV dose radiation							
	Zero		521 KJ.cm ⁻²		1042 KJ.cm ⁻²		1564 KJ.cm ⁻²	
	OMC <i>trans/cis</i>	AVO enol/keto	OMC <i>trans/cis</i>	AVO enol/keto	OMC <i>trans/cis</i>	AVO enol/keto	OMC <i>trans/cis</i>	AVO enol/keto
AVO + OMC	100.00	100.00	11.76	22.24	6.54	15.79	3.96	9.31
AVO + OMC + FA	100.00	100.00	40.67	8.90	14.75	6.45	7.71	6.19
AVO + OMC + RES	100.00	8.62	100.00	7.58	44.66	6.91	30.65	6.38

Legend: AVO, avobenzene; OMC, octyl ρ -methoxycinnamate; FA, ferulic acid; RES, resveratrol

Even before irradiation, the simple mixture of filters and RES already presented part of the AVO filter in its ketone form. However, the addition of RES preserved the *trans* OMC compared to the mixture without RES (Table II). After UV irradiation for 6 h (~1564 kJ.cm⁻²), the OMC mixed with RES showed a *trans/cis* ratio of 30.65 compared to 3.96 when no RES was added. Lower values were also observed when FA was added. Therefore, RES conserved more *trans* OMC in comparison to the FA, which suggests that RES can help photo-stabilize OMC, thereby ensuring its high absorption in the UVB wavelength range.

Suppression of singlet energy state

The absorption of photons by a chemical filter transforms them into a singlet excited state, with the electron spin remaining antiparallel. This absorbed energy may dissipate through several pathways, including intersystem crossing to the excited triplet state (parallel electron spin orientation) or vibrational relaxation (fluorescence). However, the triplet state induces the formation of singlet oxygen species on the skin surface, which causes extensive DNA damage. This is in addition to several intra- and inter-molecular photo-chemical reactions that produce molecules with the potential to cause photo-dermatosis, photo-toxicity, photo-irritation, and photo-allergic reactions.

These mechanisms are associated with reduced photo-protection efficacy (Gadgil *et al.*, 2023; Holt, Stavros, 2019).

For continued UV radiation absorption, filters must quickly return to their base state after being excited, which can be attained by inhibiting the singlet or triplet states. The singlet state inhibition can be qualitatively

analyzed by evaluating the fluorescence emission of the chemical filters. Some molecules suppress the singlet state, stabilize sun filters, and decrease its fluorescence (Kitasaka, Yagi, Kikuchi, 2020). Figure 2 shows the AVO and OMC filter singlet state suppression capacity in isolation or combination with the antioxidants FA or RES.

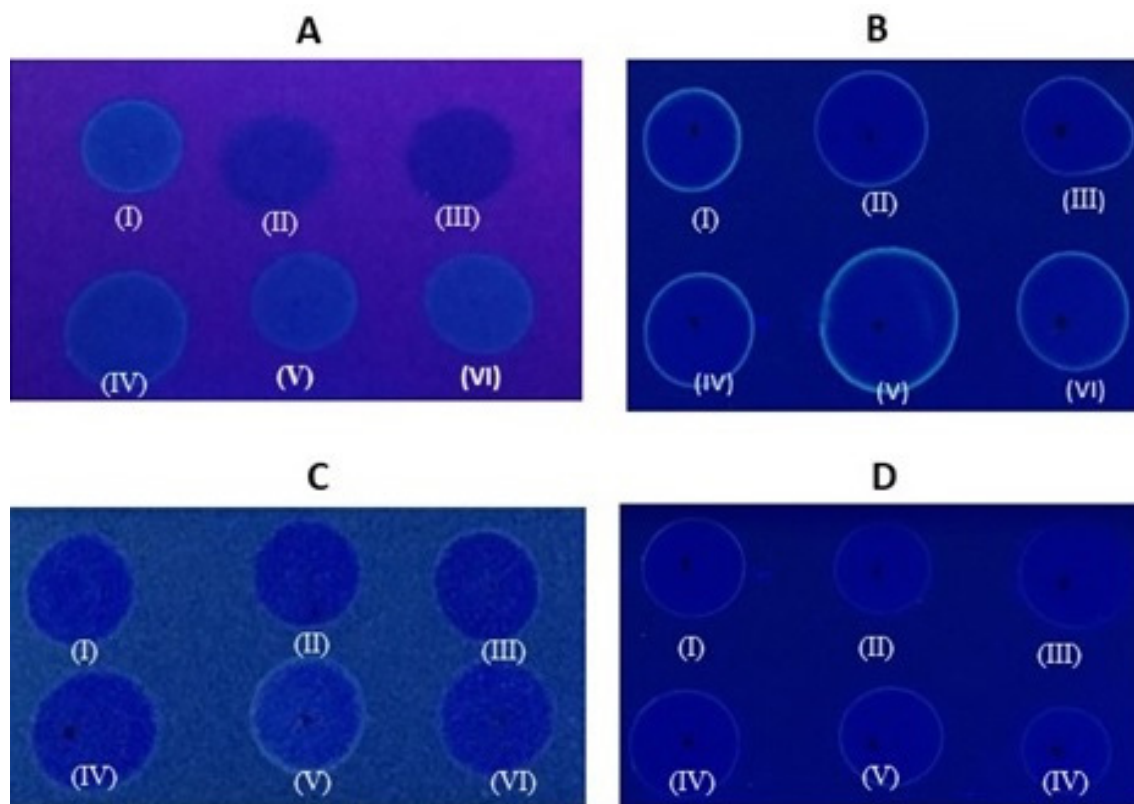


FIGURE 2 - Distribution of filter samples in methanol solution on chromatoshheet for qualitative assessment of singlet energy state suppression by FA and RES antioxidants. (A) AVO/RES; (B) AVO/FA; (C) AVO/OMC/RES; (D) AVO/OMC/FA. (I) Chemical filter; (II) Chemical filter:Antioxidant (2:1); (III) Chemical filter:Antioxidant (2:2); (IV) Chemical filter; (V) Chemical filter:phenylethylbenzoate (2:1); (VI) Chemical filter: phenylethylbenzoate (2:2).

The AVO fluorescence suppression occurred with the addition of RES in a concentration-dependent manner since the darkening was more evident when AVO was combined with RES at the ratio 2:2 compared to 2:1. The negative control was obtained by mixing the chemical filter and phenylethylbenzoate (Figure 2A-V and 2A-VI) and showed greater fluorescence intensity when compared to the solutions comprised of the filters with added RES (Figure 2A-II and 2A-III). This result was

attributed to the ability of RES to suppress the singlet excited state of AVO, thus maintaining the photo-stability of the AVO filter.

A subtle fluorescence inhibition effect was observed when both filters were added with RES (Figure 2C-I and 2C-III), although OMC did not emit fluorescence. FA did not inhibit the fluorescence of AVO, thus this antioxidant was not able to photo-stabilize AVO through singlet energy state suppression.

Stability evaluation

Formulations without antioxidants showed a statistically significant SPF reduction of 50.40, 51.02, and 63.80% when stored at 5.0, 20.0, and 45.0°C, respectively (Figure 3A). These findings were expected because higher temperatures tend to accelerate the instability and degradation processes of the formulation components (Freire *et al.*, 2019). The degradation of the chemical filters, especially OMC (UVB filter), whose reduction

in concentration was observed by qNMR, justifies these results (Figure 4B). Both antioxidants RES and FA helped maintain the SPF after 90 days of storage regardless of the storage temperature (5.0, 20.0, or 45.0°C) (Figure 3A). Thus, RES and FA mainly protected OMC (UVB filter) from thermal degradation, which potentially could maintain SPF values after UV radiation exposure, as was observed for the flavonoid rutin when added to sunscreen (Pinto *et al.*, 2021).

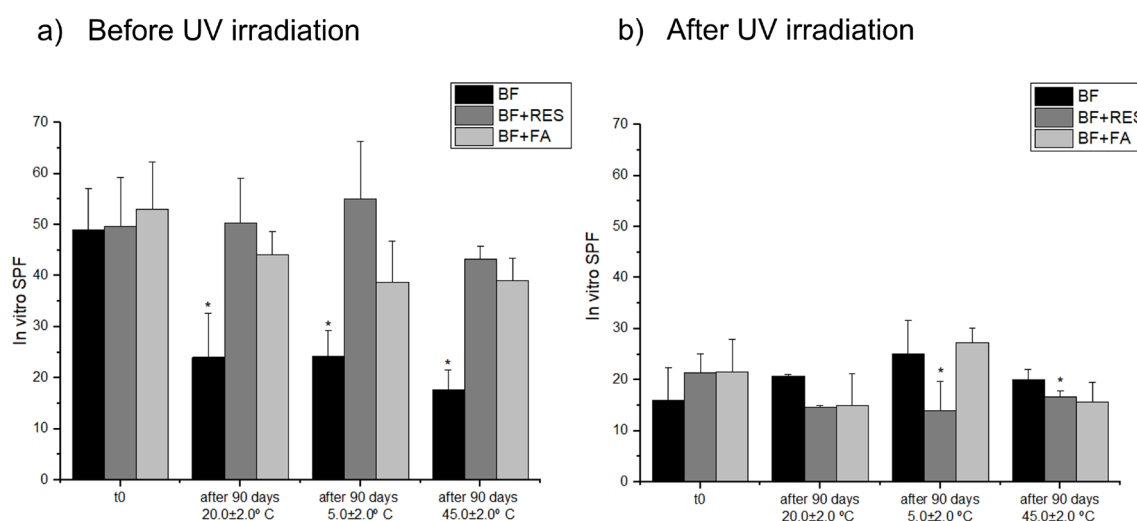


FIGURE 3 - In vitro Sun Protection Factor (SPF) of formulations in Thermal Stability Test (a) and Photostability Test (b).

Legend: BF, base formulation; RES, resveratrol; FA, ferulic acid. $t_0 = 48$ h after preparing the formulations. Results that are statistically different by paired t-test were represented by one asterisk ($\alpha = 0.05$).

However, the photo-stability assay showed that UV radiation reduced the SPF of all formulations independent of their different previous storage conditions, indicating that adding FA or RES did not benefit the photo-stability of the sunscreen (Figure 3B).

The critical wavelength ($\lambda_{\text{critical}}$) remained above 370 nm for all formulations during the thermal stability and photo-stability tests, thereby maintaining this broad-spectrum characteristic (Galdi *et al.*, 2022). However, after UV exposure, the $\lambda_{\text{critical}}$ parameter of all formulations was reduced ($p \leq 0.05$), despite

maintaining the minimum value of 370 nm. Thus, the addition of antioxidants did not substantially influence this parameter. The same pattern was observed for the UVA/UVB ratio since the addition of flavonoids was not able to protect the formulation. The decrease in both values suggests a reduction in UVA protection, which can be explained by the degradation of AVO (UVA filter) shown in Figure 4A. The UVA/UVB ratio decreased over 90 days; however, in this study it was considered adequate as it was between 0.6 and 0.95 (Galdi *et al.*, 2022; Moyal, 2012).

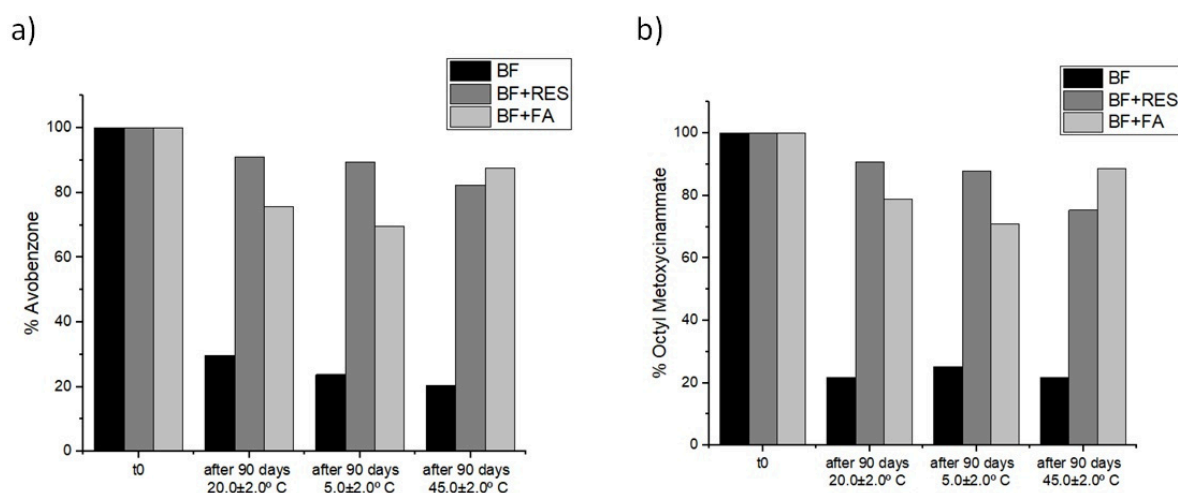


FIGURE 4 - Quantitative Nuclear Magnetic Resonance (qNMR) of chemical filters in sunscreens formulations.

Legend: BF, base formulation; RES, resveratrol; FA, ferulic acid; t_0 = 48h after preparing the formulations.

Porcine ear skin penetration/permeation assessment

The receptor fluid was based on PBS pH 7.4 containing 4.0% BSA, for its high ability to solubilize lipophilic molecules and to avoid false results due to insufficient UV filter solubility. It is known that the composition of the receptor fluid significantly

affects the percutaneous permeation test (Klimová, Hojerová, Beránková, 2015). The addition of other compounds, such as 20% ethanol, was evaluated, but filter solubility was not improved (data not shown). Table III and Figure 5 show the chemical filter (AVO and OMC) concentrations on the skin surface and in each component (stratum corneum and epidermis plus dermis) beyond the receptor liquid.

TABLE III - Distribution of the UV filters after 24 h exposure of pig ear skin to sunscreens

Component of the diffusion system	BF		BF + RES		BF + FA	
	AVO	OMC	AVO	OMC	AVO	OMC
Surface ($\text{mg}\cdot\text{cm}^{-2}$)	3.73 ± 0.22	7.52 ± 0.32	3.40 ± 0.08	7.14 ± 0.11	3.99 ± 0.08	8.52 ± 0.19
Stratum corneum ($\text{mg}\cdot\text{cm}^{-2}$)	0.08 ± 0.00	0.03 ± 0.00	0.00 ± 0.00	0.03 ± 0.00	0.00 ± 0.00	0.03 ± 0.00
Epidermis + Dermis ($\text{mg}\cdot\text{cm}^{-2}$)	0.10 ± 0.00	0.06 ± 0.01	0.02 ± 0.00	0.10 ± 0.00	0.00 ± 0.00	0.05 ± 0.00
Receptor fluid ($\text{mg}\cdot\text{cm}^{-2}$)	0.00 ± 0.00	0.00 ± 0.00	0.00 ± 0.00	0.00 ± 0.00	0.00 ± 0.00	0.00 ± 0.00
Recovery (% w/w)	92.13 ± 5.25	89.64 ± 3.95	85.59 ± 2.17	85.71 ± 1.31	94.14 ± 1.94	101.59 ± 2.22

Legend: BF, base formulation; AVO, avobenzone; OMC, octyl p-methoxycinnamate; FA, ferulic acid; RES, resveratrol

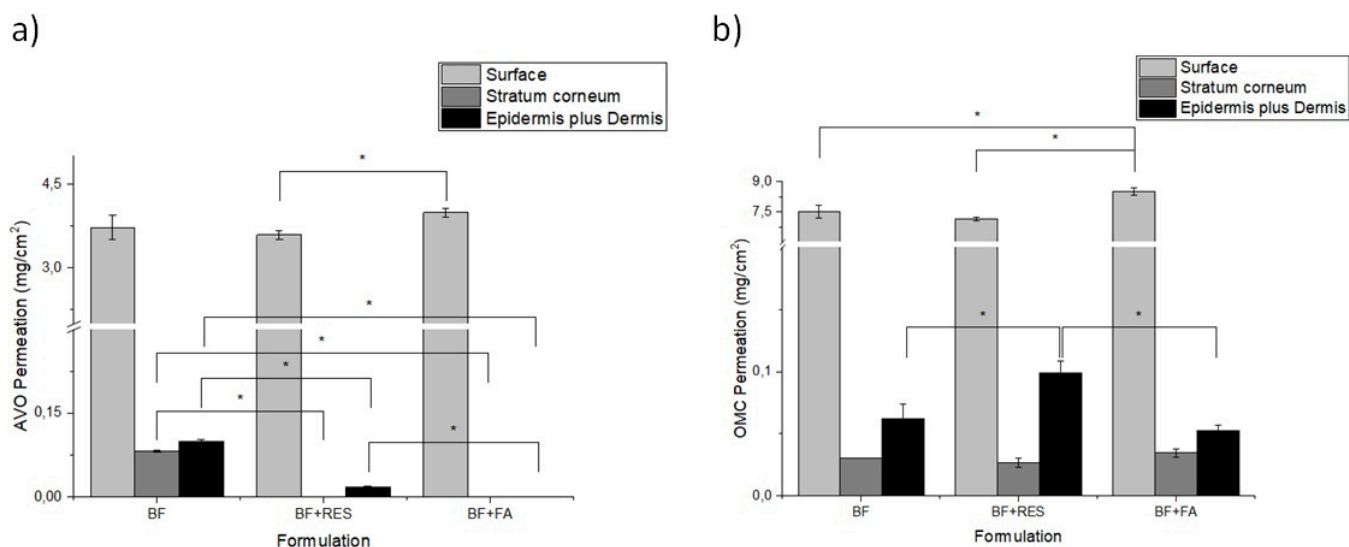


FIGURE 5 - Permeation of the UV filters on the pig ear skin.

Legend. BF, base formulation; RES, resveratrol; FA, ferulic acid; AVO, avobenzone; OMC, octyl *p*-methoxycinnamate. Asterisks identify statistically significant differences by ANOVA one way followed by the Tukey's test ($\alpha = 0.05$)

Sunscreens are expected to remain on the skin surface to protect it against the negative effects of the sun by absorbing, reflecting, or scattering UV radiation. In addition, their permeation must be avoided to decrease the risks of topical or systemic toxicity due to photo-allergic reactions or the endocrine disrupting properties of some UV filters, to cite a few examples of the potential harmful effects. This study showed that >95% of the UV filters applied to the pig ear skin did not penetrate but were retained on the skin surface. When incorporated into the base formulation, a small amount of AVO and OMC were able to penetrate the skin because they were quantified in the stratum corneum (2nd–14th tape) and the viable skin layers (epidermis plus dermis). Fick's first law states that the permeation of a topically administered drug is correlated to the difference between the concentration of a drug in the vehicle and the skin (Iyer *et al.*, 2021). However, the physicochemical properties of the drugs, such as lipophilicity ($\log P$), molecular weight (MW), melting point (MP), and topological polar surface area (TPSA), in addition to the interactions between the drug and vehicle, also significantly affect the permeability coefficient (Neupane *et al.*, 2020). According to Ates *et al.* (2016), compounds that meet these criteria are

more likely to permeate the skin: MW <180 Da and/or $\log P \geq 0.3$ and/or MP <100°C and/or TPSA <40 Å². However, MW is considered a stricter barrier for molecules that are >500 Da (Iyer *et al.*, 2021).

Skin permeation may be achieved via three pathways: transcellular (chemicals diffuse through the intracellular spaces of corneocytes), intercellular (chemicals diffuse through the lipid-rich extracellular regions around the corneocytes), and transappendageal (chemicals enter via the hair follicles, sweat glands, and sebaceous glands). In both the transcellular and intercellular pathways, the drug must diffuse first into the intercellular lipid matrix in the stratum corneum, which is considered the major determinant of drug permeation by the skin.

Some physicochemical properties of OMC and AVO contribute to their transcellular/intercellular penetration, namely: MW, $\log P$, MP, and TPSA (Table IV). The TPSA of AVO is the single criterion that is not completely met and impairs its transcellular/intercellular permeation. However, according to Munem *et al.* (2021), AVO is mainly transported via the appendageal route (specifically the follicular transport route with the sebaceous gland acting as the reservoir), which is considered of minor importance because these follicles account for about 0.1% of the total skin surface (Pereira *et al.*, 2021).

TABLE IV - Physicochemical compound parameters

Physicochemical parameter	OMC	AVO	RES	FA
Molecular weight (Da)	290.4	310.4	228.24	194.18
log P	6.10	4.51	3.10	1.51
Melting point (° C)	-25	83.5	253–255	168–171
TPSA (Å ²)	35.5	43.4	60.7	66.8

Legend: AVO, avobenzonone; OMC, octyl p-methoxycinnamate; FA, ferulic acid; RES, resveratrol; TPSA, topological polar surface area

Thus, although most physicochemical parameters contribute to the permeation of chemical filters, this occurs to a small extent due to the interaction between the compound and vehicle (an oil-in-water emulsion) and its high viscosity, which hinders its release from the formulation. Previous studies have shown low skin permeation in both human and porcine skin models (Freitas *et al.*, 2015; Montenegro *et al.*, 2018; Munem *et al.*, 2021; Pafili *et al.*, 2021), which is in agreement with our results.

The addition of RES and FA was accompanied by a reduction in AVO penetration/permeation; however, FA was more efficient than RES. Regarding the OMC filter, it was observed that RES caused an increase in its permeation while FA showed no impact. RES is poorly soluble in water (<0.05 mg/mL) but is highly soluble in OMC, as demonstrated by thermal analysis (Freire *et al.*, 2022). Thus, the obtained results might be explained by the high chemical affinity between OMC and RES, which could reduce its release from the formulation and its chemical penetration into the stratum corneum (Delmas *et al.*, 2011; Ellison *et al.*, 2020).

After 24 h of the permeation study, the AVO and OMC chemical filters were not quantified in the receptor liquid, which indicates that all formulations could be considered safe because no systemic absorption is expected (Adamson, Shinkai, 2020). The total recovery of all the studied filters were within the range of 85–115% as recommended by the Scientific Committee on Consumer Safety (SCCS, 2021).

CONCLUSIONS

The addition of RES and FA induces positive changes in the efficacy and safety profiles of sunscreens, in addition to their antioxidant activity. Thus, further studies are required to establish the real cost–benefit ratio for their use in these formulations.

ACKNOWLEDGMENTS

This work was supported by Fundação de Amparo à Pesquisa do Estado de São Paulo – Fapesp (Project 2018/11073-2), Brazil, and Coordenação de Aperfeiçoamento de Pessoal de Nível Superior – CAPES (grant number 88882.377642/2019-01), Brazil.

REFERENCES

- Adamson AS, Shinkai K. Systemic Absorption of Sunscreen. *JAMA*. 2020;323:223. <https://doi.org/10.1001/jama.2019.20143>.
- ANVISA. RDC nº 600, de 9 de fevereiro de 2022. Dispõe sobre a lista de filtros ultravioletas permitidos para produtos de higiene pessoal, cosméticos e perfumes e internaliza a Resolução GMC MERCOSUL no 44/2015, alterada pela Resolução GMC MERCOSUL no 14/2021. 2022.
- Ates G, Steinmetz FP, Doktorova TY, Madden JC, Rogiers V. Linking existing in vitro dermal absorption data to physicochemical properties: Contribution to the design of a weight-of-evidence approach for the safety evaluation of cosmetic ingredients with low dermal bioavailability. *Regul Toxicol Pharmacol*. 2016;76:74–8. <https://doi.org/10.1016/j.yrtph.2016.01.015>.

- Barresi R, Chen E, Liao I-C, Liu X, Baalbaki N, Lynch S, et al. Alteration to the Skin Barrier Integrity Following Broad-spectrum UV Exposure in an Ex vivo Issue Model. *J Drugs Dermatol.* 2021;20:23–8.
- Batista IASA, Gonçalves MIDA, Singh AK, Hackmann ERK, Santoro MIRM. Quantitative Determination of Dimethylaminoethanol in Cosmetic Formulations by Nuclear Magnetic Resonance Spectroscopy. *JAOAC Int.* 2008;91:1303–8. <https://doi.org/10.1093/jaoac/91.6.1303>.
- Berenbeim JA, Wong NGK, Cockett MCR, Berden G, Oomens J, Rijs AM, et al. Unravelling the Keto–Enol Tautomer Dependent Photochemistry and Degradation Pathways of the Protonated UVA Filter Avobenzone. *J Phys Chem A.* 2020;124:2919–30. <https://doi.org/10.1021/acs.jpca.0c01295>.
- Bonda CA. Test method for determining compounds capable of quenching electronic singlet state excitation of photoactive compounds. WO-2009020673-A1, 2009.
- Delmas D, Aires V, Limagne E, Dutartre P, Mazué F, Ghiringhelli F, et al. Transport, stability, and biological activity of resveratrol. *Ann N Y Acad Sci.* 2011;1215:48–59. <https://doi.org/10.1111/j.1749-6632.2010.05871.x>.
- Ellison CA, Tankersley KO, Obringer CM, Carr GJ, Manwaring J, Rothe H, et al. Partition coefficient and diffusion coefficient determinations of 50 compounds in human intact skin, isolated skin layers and isolated stratum corneum lipids. *Toxicol In Vitro.* 2020;69:104990. <https://doi.org/10.1016/j.tiv.2020.104990>.
- Freire TB, Lima CRRC, Pinto CASO, Borge LF, Baby AR, Velasco MVR. Evaluation of interaction between natural antioxidants and chemical sunscreens aiming the photoprotective efficacy. *J Therm Anal Calorim.* 2022;147:7829–36. <https://doi.org/10.1007/s10973-021-11111-8>.
- Freire TB, Dario MF, Mendes OG, Oliveira AC, Vetore-Neto A, Faria DLA, et al. Nanoemulsion containing caffeine for cellulite treatment: characterization and in vitro evaluation. *Braz J Pharm Sci.* 2019;55. <https://doi.org/10.1590/s2175-97902019000218236>.
- Freitas JV, Praça FSG, Bentley MVLB, Gaspar LR. Trans-resveratrol and beta-carotene from sunscreens penetrate viable skin layers and reduce cutaneous penetration of UV-filters. *Int J Pharm.* 2015;484:131–7. <https://doi.org/10.1016/j.ijpharm.2015.02.062>.
- Gadgil VR, Darak A, Patil SJ, Chopada A, Kulkarni RA, Patil SM, et al. Recent developments in chemistry of sunscreens & their photostabilization. *J Indian Chem Soc.* 2023;100:100858. <https://doi.org/10.1016/j.jics.2022.100858>.
- Galdi A, Foltis P, Bodnar B, Moyal D, Oresajo C. Sunscreens. *Cosmetic Dermatology*, Wiley; 2022, p. 204–11. <https://doi.org/10.1002/9781119676881.ch21>.
- Herzog B, Amorós-Galicia L, Sohn M, Hofer M, Quass K, Giesinger J. Analysis of photokinetics of 2'-ethylhexyl-4-methoxycinnamate in sunscreens. *Photochem Photobiol Sci.* 2019;18:1773–81. <https://doi.org/10.1039/c9pp00084d>.
- Herzog B, Giesinger J, Settels V. Insights into the stabilization of photolabile UV-absorbers in sunscreens. *Photochem Photobiol Sci.* 2020;19:1636–49. <https://doi.org/10.1039/d0pp00335b>.
- Holt EL, Stavros VG. Applications of ultrafast spectroscopy to sunscreen development, from first principles to complex mixtures. *Int Rev Phys Chem.* 2019;38:243–85. <https://doi.org/10.1080/0144235X.2019.1663062>.
- Holzgrabe U, Deubner R, Schollmayer C, Waibel B. Quantitative NMR spectroscopy—Applications in drug analysis. *J Pharm Biomed Anal.* 2005;38:806–12. <https://doi.org/10.1016/j.jpba.2005.01.050>.
- Iyer A, Vaskuri GSSJ, Agrawal A, Khatri D, Srivastava S, Singh S, et al. Does skin permeation kinetics influence efficacy of topical dermal drug delivery system?: Assessment, prediction, utilization, and integration of chitosan biomacromolecule for augmenting topical dermal drug delivery in skin. *J Adv Pharm Technol Res.* 2021;12:345. https://doi.org/10.4103/japtr.japtr_82_21.
- Jiménez MM, Pelletier J, Bobin MF, Martini MC. Influence of encapsulation on the in vitro percutaneous absorption of octyl methoxycinnamate. *Int J Pharm.* 2004;272:45–55. <https://doi.org/10.1016/j.ijpharm.2003.11.029>.
- Kitasaka S, Yagi M, Kikuchi A. Suppression of menthyl anthranilate (UV-A sunscreen)-sensitized singlet oxygen generation by Trolox and α -tocopherol. *Photochem Photobiol Sci.* 2020;19:913–9. <https://doi.org/10.1039/d0pp00023j>.
- Klimová Z, Hojerová J, Beránková M. Skin absorption and human exposure estimation of three widely discussed UV filters in sunscreens – In vitro study mimicking real-life consumer habits. *Food Chem Toxicol.* 2015;83:237–50. <https://doi.org/10.1016/j.fct.2015.06.025>.
- Kojic M, Petkovic M, Etinski M. Unrevealing mechanism of the thermal tautomerization of avobenzone by means of quantum chemical computations. *J Serb Chem Soc.* 2016;81:1393–406. <https://doi.org/10.2298/JSC160531085K>.
- Montenegro L, Turnaturi R, Parenti C, Pasquinucci L. In vitro evaluation of sunscreen safety: effects of the vehicle and repeated applications on skin permeation from topical formulations. *Pharmaceutics.* 2018;10:27. <https://doi.org/10.3390/pharmaceutics10010027>.

- Moyal D. The development of efficient sunscreens. *Indian J Dermatol Venereol Leprol.* 2012;78:31. <https://doi.org/10.4103/0378-6323.97353>.
- Munem M, Djuphammar A, Sjölander L, Hagvall L, Malmberg P. Animal-free skin permeation analysis using mass spectrometry imaging. *Toxicol in Vitro.* 2021;71:105062. <https://doi.org/10.1016/j.tiv.2020.105062>.
- Murphy RB, Staton J, Rawal A, Darwish TA. The effect of deuteration on the keto–enol equilibrium and photostability of the sunscreen agent avobenzone. *Photochem Photobiol Sci.* 2020;19:1410–22. <https://doi.org/10.1039/d0pp00265h>.
- Neupane R, Boddu SHS, Renukuntla J, Babu RJ, Tiwari AK. Alternatives to Biological Skin in Permeation Studies: Current Trends and Possibilities. *Pharmaceutics.* 2020;12:152. <https://doi.org/10.3390/pharmaceutics12020152>.
- Pafili A, Meikopoulos T, Kontogiannidou E, Papageorgiou S, Demiri E, Meimari D, et al. Development and validation of LC-MS/MS method for the determination of UV-filters across human skin in vitro. *J Chromatogr B.* 2021;1167:122561. <https://doi.org/10.1016/j.jchromb.2021.122561>.
- Pereira R, Silva SG, Pinheiro M, Reis S, Vale ML. Current status of amino acid-based permeation enhancers in transdermal drug delivery. *Membranes (Basel).* 2021;11:343. <https://doi.org/10.3390/membranes11050343>.
- Peres DD, Sarruf FD, Oliveira CA, Velasco MVR, Baby AR. Ferulic acid photoprotective properties in association with UV filters: multifunctional sunscreen with improved SPF and UVA-PF. *J Photochem Photobiol B.* 2018;185:46–9. <https://doi.org/10.1016/j.jphotobiol.2018.05.026>.
- Pinto CASO, Gonçalves MIA, Martins TEA, Issa MG, Lima FS, Costa GMD, et al. Rutin as photostabilizer for broad spectrum sunscreens. *Braz J Dev.* 2021;7:92115–32. <https://doi.org/10.34117/bjdv7n9-397>.
- Rojas J, Londono C, Ciro Y. The health benefits of natural skin UVA photoprotective compounds found in botanical sources. *Int J Pharm Pharm Sci.* 2016;8:13–23.
- SCCS. Scientific Committee on Consumer Safety. The SCCS's Notes of Guidance for the Testing of Cosmetic Substances and Their Safety Evaluation. 11th Revision. SCCS/1628/21, p. 31. 2021. https://health.ec.europa.eu/system/files/2022-08/sccs_o_250.pdf (accessed January 26, 2023).
- Serpone N. Sunscreens and their usefulness: have we made any progress in the last two decades? *Photochem Photobiol Sci.* 2021;20:189–244. <https://doi.org/10.1007/s43630-021-00013-1>.
- Union P. Regulation (EC) n° 1223/2009 of the European Parliament and of the Council. *Off J Eur Union.* 2009;342:59.
- WHO. Radiation: Ultraviolet (UV) radiation and skin cancer 2017. [https://www.who.int/news-room/q-a-detail/radiation-ultraviolet-\(uv\)-radiation-and-skin-cancer](https://www.who.int/news-room/q-a-detail/radiation-ultraviolet-(uv)-radiation-and-skin-cancer) (accessed August 1, 2021).
- Zhang Y-Y, Zhang J, Zhang W-X, Wang Y, Wang Y-H, Yang Q-Y, et al. Quantitative 1H Nuclear Magnetic Resonance Method for Assessing the Purity of Dipotassium Glycyrrhizinate. *Molecules* 2021;26:3549. <https://doi.org/10.3390/molecules26123549>.

Received for publication on 13rd June 2023

Accepted for publication on 20th July 2023